ACS APPLIED MATERIALS & INTERFACES

www.acsami.org Research Article

Cucurbit[7]uril-Mediated 2D Single-Layer Hybrid Frameworks Assembled by Tetraphenylethene and Polyoxometalate toward Modulation of the α-Chymotrypsin Activity

Ni Cheng, Yong Chen, Yi Zhang, and Yu Liu*

Cite This: *ACS Appl. Mater. Interfaces* 2020, 12, 15615−15621 Read Online

ACCESS | Metrics & More | Article Recommendations | Supporting Information

ABSTRACT: Construction of large-scale single-layer two-dimensional (2D) frameworks in water is significant due to their utilities in various fields. Utilizing macrocycle-mediated supramolecular self-assembly represents a promising approach; however, challenges still remain in their practical preparation. Here, we exploited a two-step supramolecular strategy to build 2D organic−inorganic hybrid frameworks at a micrometer scale in water. Taking advantage of the high binding affinity to cucurbit[7]uril (CB[7]), mono-quaternary ammonium tetraphenylethene (MQATPE) derivatives were first included with CB[7] to form a 1:1 complex (MQATPE@CB[7]). Then, just mixing the complex with anionic polyoxometalate $Na_9[EuW_{10}O_{36}]\cdot 32H_2O$ (denoted as Eu-POM) in a 3:1 molar ratio leads to the formation of single-layer 2D films with tens of micrometers via electrostatic and π−π stacking interactions. The most unique feature of this strategy is that the steric effect imposed by CB[7] would not only lead the modules to adopt a periodic hexagonal assembly but also forbid stacking between layers through comparison with the merely multilayered 2D nanosheets self-assembled by MQATPE/Eu-POM. Interestingly, the charge interactions between MQATPE and Eu-POM would lead to the aggregation-induced emission (AIE) fluorescence of MQATPE, and white light emission could be obtained through the simple regulation of the contents of Eu-POM and MQATPE. Furthermore, due to the high surface areas and more accessible active sites, the single-layer films can act as an effective enzyme inhibitor to modulate the activity of α-chymotrypsin (ChT). These findings suggest a simple but universal approach for single-layer hybrid materials, which may hold promise for practical applications in photophysical and biomedical fields.

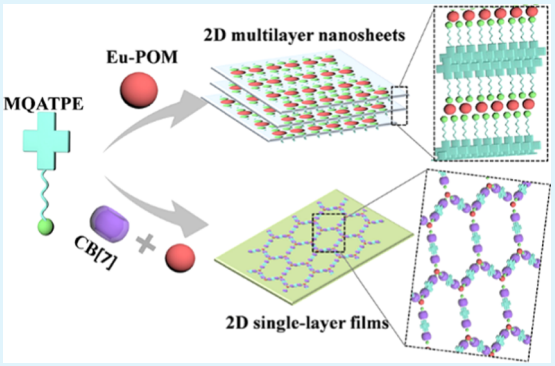

KEYWORDS: *2D frameworks, single layer, cucurbit[7]uril, tetraphenylethene, polyoxometalate*

INTRODUCTION

Two-dimensional (2D) frameworks are contemporary materials that have received tremendous attention because of their superior properties originating from their highly accessible active sites.[1,2] 2D frameworks have been successfully applied in the fields of membrane separation,[3,4] biomedicine,[5] energy storage,[6] and sensing.[7] As a type of 2D framework, single-layer 2D framework holds great promise in terms of better performance than multilayers.[8−11] Although tremendous progress has been made to obtain single-layer 2D frameworks, big challenges still remain owing to the rational structural design, complicated synthetic methodology, and especially strong interlayer but weak inlayer interactions.[12] Furthermore, the search for molecularly thin 2D frameworks with diverse compositions and functionalities has become a hot research topic. Organic−inorganic hybrid supramolecular structures possess enormous physicochemical properties and structural versatility.[13] Therefore, a rapid method to controllably construct hybrid single-layer 2D frameworks in solution is still highly desired.

Supramolecular self-assembly based on intermolecular noncovalent interactions is a promising approach to fabricate ordered structure due to the significant advantages such as facile construction and inherently self-correcting properties.[14−16] Among them, macrocycle-mediated assemblies especially provide opportunities to fabricate various 2D frameworks.[17,18] For example, Li's and Feng's groups have developed a single-layer 2D honeycomb supramolecular organic framework through cucurbit[8]uril inclusion interaction.[12,39] Our group has reported a series of macrocycle-mediated supramolecular 2D nanoassemblies with structural and functional diversities.[20−23] Although promising results

Received: February 16, 2020
Accepted: March 5, 2020
Published: March 5, 2020

Downloaded via NANKAI UNIV on August 30, 2020 at 03:05:24 (UTC).
See https://pubs.acs.org/sharingguidelines for options on how to legitimately share published articles.

ACS Publications © 2020 American Chemical Society

https://dx.doi.org/10.1021/acsami.0c02976
ACS Appl. Mater. Interfaces 2020, 12, 15615−15621

have been achieved with 2D organic assemblies, little has been achieved in the construction of supramolecular single-layer hybrid 2D frameworks in the solution phase.

Polyoxometalates (POMs) as a kind of discrete metal-oxide clusters have been proved to be outstanding candidates for supramolecular self-assembly owing to their rich architecture and multiple negative charges.[24−26] Wu and co-workers constructed single-layer 2D frameworks by pseudorotaxane and POMs cluster nodes in water for pinpoint size-selective separation.[27] Although design and applications of 2D frameworks are explored in diverse biomedical fields, few researchers are focused on the modulation of enzyme activity using hybrid single-layer 2D frameworks. Their several advantages such as ease of synthesis, large surface area, and functional surface can provide influential means to enhance the modulation activity.

Herein, we present a cucurbit[7]uril (CB[7])-mediated strategy to simply construct 2D hybrid single-layer frameworks with large size and regular shape in the water. The basic self-assembly concepts are illustrated in Scheme 1: mono-

Scheme 1. Construction of 2D Hybrid Single-Layer Frameworks via Self-Assembly of Cationic MQATPE@CB[7] and Anionic Eu-POM

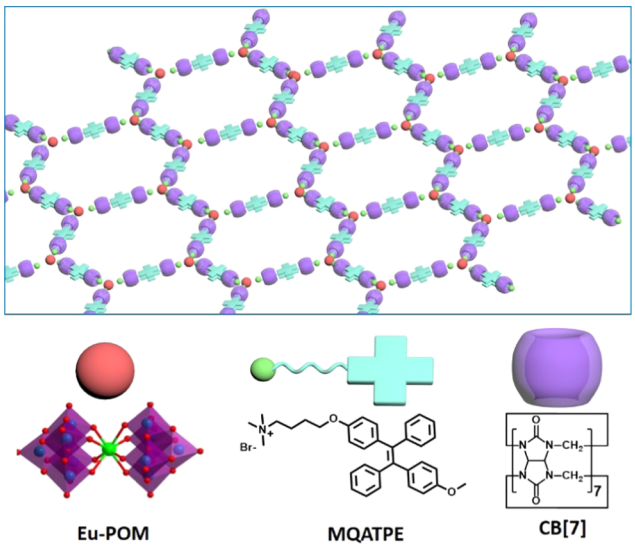

quaternary ammonium tetraphenylethene (MQATPE)@CB[7] was employed as the organic linker and Eu-POM as connection nodes. Upon $\pi-\pi$ stacking between TPE groups and electrostatic interaction among cationic ammonium and polyanionic Eu-POM clusters, 2D supramolecular hybrid single-layer 2D frameworks were constructed. The steric effect imposed by macrocycle CB[7] on the alkyl chain would lead to the periodic hexagonal single-layer films with a lateral size as large as several tens of micrometers. Interestingly, through simple regulation of the contents of the red-emitting Eu-POM and blue-emitting MQATPE, the white-light-emitting mixture could be obtained. More significantly, due to the high surface areas and more accessible active sites, the single-layer films can act as an effective enzyme inhibitor to modulate the activity of α-chymotrypsin (ChT).

■ RESULTS AND DISCUSSION

MQATPE and Eu-POM were prepared according to the previous reports.[28,29] As well-documented, CB[7] enables to internalize alkyl chain bearing cationic ammonium to form 1:1 binary complexes, with the association constant as high as 10^6 M^{-1}.[30] In this work, binary inclusion complex MQATPE@CB[7] was constructed by adding equal molar ratio of CB[7] into the MQATPE solution. As observed from Figure 1, the

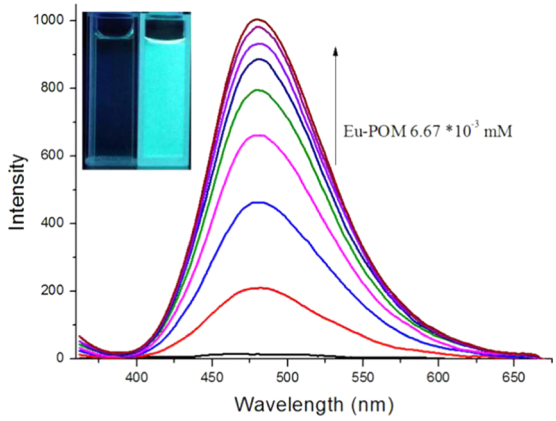

Figure 1. Fluorescence spectra of MQATPE with the addition of Eu-POM in an aqueous solution (λ_{ex} = 350 nm). The concentration of MQATPE was fixed at 2.5×10^{-2} mM and the concentration of Eu-POM was varied from 0 to 6.67×10^{-3} mM.

solution of MQATPE barely fluoresces nor does it after the CB[7] solution has been added (Figure S1), indicating that no restriction of the intramolecular rotation of the phenyl rings occurred.[31] When the Eu-POM solution was gradually added to the MQATPE solution, the fluorescence intensity of MQATPE was greatly enhanced, with the fluorescence clearly observable by the naked eye. We deduced that the enhanced fluorescence was attributed to the existence of charge interactions between the cationic ammonium group on MQATPE and the anionic charged Eu-POM, thus inducing the aggregation of MQATPE, which consequently led to the aggregation-induced emission (AIE) fluorescence of MQATPE.

The Eu-POM can emit red fluorescence when excited at 280 nm due to the intramolecular energy transfer from the ligand-to-metal charge-transfer (LMCT) band of heteropolyoxotung to the Eu^{3+} core.[32] The photoluminescent properties of Eu-POM with the gradual addition of MQATPE@CB[7] were researched. As shown in Figure 2, the pure Eu-POM solution displays obvious characteristic transitions of Eu^{3+}: $^5D_0-^7F_0$ at 576 nm, $^5D_0-^7F_1$ at 590 nm, $^5D_0-^7F_2$ at 617 nm, $^5D_0-^7F_3$ at 649 nm, and $^5D_0-^7F_4$ at 697 nm. With the increase of MQATPE@CB[7], the fluorescence intensity of Eu-POM is partly quenched. The quenching of Eu-POM could be ascribed to the ammonium group of MQATPE, which would block the energy transfer from the O/W LMCT states to the Eu^{3+} ion in the first step. As the $^5D_0-^7F_2$ transition is sensitive to the chemical environments around Eu^{3+} ions, while the $^5D_0-^7F_1$ transition is almost independent of the changes, the intensity ratio of $I(^5D_0-^7F_2)/I(^5D_0-^7F_1)$ could be used to analyze the chemical microenvironments of Eu^{3+} ions.[33] This ratio in the presence of MQATPE@CB[7] is lower than that of pure Eu-POM, indicating the increased symmetrical environment of Eu-POM in the complex. These phenomena could be attributed to the fact that MQATPE@CB[7] has gradually replaced the coordinate water due to the strong electrostatic interactions between Eu-POM and ammonium segments.[32]

https://dx.doi.org/10.1021/acsami.0c02976
ACS Appl. Mater. Interfaces 2020, 12, 15615−15621

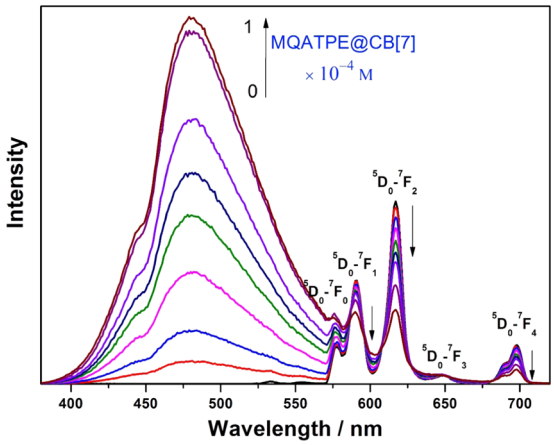

Figure 2. Emission spectra of the mixture of Eu-POM and MQATPE@CB[7] in aqueous solution (λ_{ex} = 280 nm). The concentration of Eu-POM was fixed at 1.25 × 10^{-4} M and the concentration of MQATPE@CB[7] was varied from 0 to 1 × 10^{-4} M.

These luminescent properties of Eu-POM were consistent with the gradual addition of only MQATPE (Figure S2), which confirms the fact that the existence of CB[7] molecule would have little effect on the original electrostatic interactions.

Upon excitation with 280 nm light, the CIE coordinates (Figure 3) of (0.62, 0.38) for the Eu-POM solution are close to

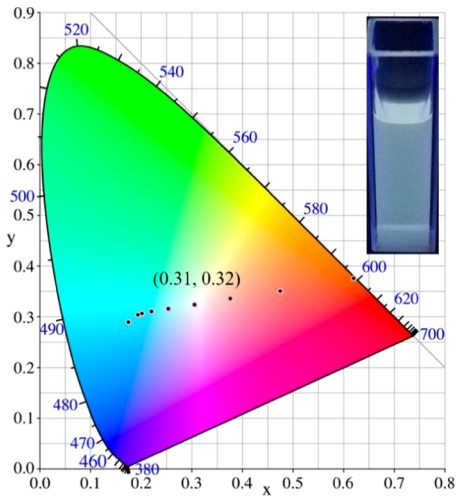

Figure 3. CIE coordinates of MQATPE@CB[7] and Eu-POM mixture excited at 280 nm.

those of (0.66, 0.33) for the saturated red emitter.[34] With the introduction of MQATPE@CB[7] to the Eu-POM solution, the fluorescence intensity of MQATPE is gradually enhanced and the blue emission intensity of the mixture was improved significantly. The emission spectrum of the mixture covers almost the whole visible spectral region (400−720 nm) when excited at 280 nm. Blending MQATPE@CB[7] and Eu-POM in the mole ratio of 1:8.33 led to white emission (inserted photograph) with CIE coordinates of (0.31, 0.32), close to those of the ideal white light.

Scanning electron microscopy (SEM) images showed that the free MQATPE gave rise to nanoparticle morphology with dozens of nanometers (Figure S3a). With increasing the molar fraction of MQATPE and Eu-POM from 1:1 to 9:1, the morphologies transform from giant particles hundreds nanometer to 2D planar flakes with the lateral dimension of several micrometers (Figures 4a and S3b−d). The SEM images

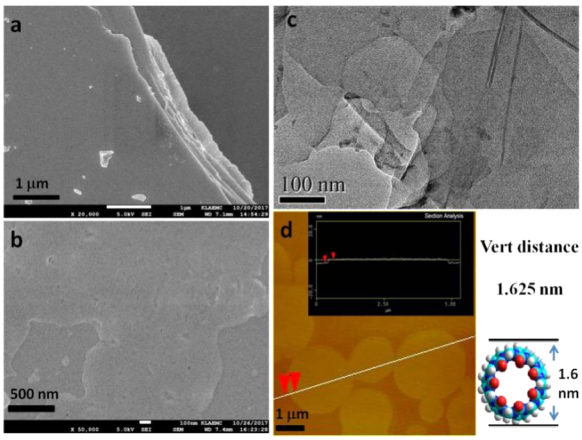

Figure 4. Morphological observations of the 2D nanostructures: (a) SEM image of MQATPE + Eu-POM assembly, (b) SEM, (c) TEM, and (d) AFM images of MQATPE@CB[7] + Eu-POM assembly (MQATPE@CB[7] = 2.5 × 10^{-5} M, the molar ratio of MQATPE to Eu-POM was fixed at 3:1).

(Figure 4b) demonstrate the three MQATPE@CB[7] + Eu-POM component systems present extended 2D films with large lateral dimensions. Such films seem to have a uniform thickness, since no multiple 2D sheets stack on each other, as observed in the images of the MQATPE/Eu-POM assembly. In the transmission electron microscopy (TEM), these three-component 2D films are very thin as observed by diaphanous morphology when they overlap (Figure 4c). The energy-dispersive X-ray (EDX) spectral analysis of the observed films points out the presence of europium and tungsten elements (Figure S4), confirming the existence of clusters in the films. The atomic force microscopy (AFM) studies confirmed the above results even more clearly. As shown in Figures 4d and S5, the film thickness is homogeneous in areas at the micrometer scale as expected and the thickness is determined to be around 1.6−1.7 nm. The thickness is consistent with the outer diameter of CB[7], indicating that single-layer films have been successfully fabricated.

FTIR and Raman spectroscopies are useful tools to demonstrate the driving force interactions for the assembly. In the FTIR spectrum of Eu-POM (Figure S6), four characteristic vibration peaks were determined: 929 cm^{-1} assigned to ν(W = Od), 833 cm^{-1} assigned to ν(W−Ob−W), and 771 and 684 cm^{-1} assigned to ν(W−Oc−W).[35] After the complexation with MQATPE, these four bands in the nanocomposite sheets are preserved. These results demonstrate that Eu-POM clusters have been incorporated into the nanosheets with the basic structure preserved. The slight shifts at 771 and 684 cm^{-1} demonstrate the existence of electrostatic interaction between MQATPE and Eu-POM.[26] In the MQATPE@CB[7] + Eu-POM films, the four characteristic vibrations (including the shifts) of Eu-POM and the vibrations of CB[7] are all presented in the spectrum, which confirm the existence of CB[7] in the films and the CB[7] molecule would have little effect on the original electrostatic interactions.

In the Raman spectra of the films in Figure S7, the W═O symmetric stretching vibration band at 970 cm^{-1} shifts to 964 cm^{-1}, the W_2−O corner-sharing band at 892 shifts to 900 cm^{-1}, and the W_3−O stretching vibration band at 553 shifts to

https://dx.doi.org/10.1021/acsami.0c02976
ACS Appl. Mater. Interfaces 2020, 12, 15615−15621

572 cm^{-1}. Meanwhile, the stretching vibration of CB[7] in the films is consistent with that of pure CB[7]. These results further prove that Eu-POMs are incorporated into the assembly through the electrostatic interactions with MQATPE molecules, which would not be destroyed by the existence of CB[7] molecules.

The ordered structures were investigated by powder X-ray diffraction (XRD) measurements (Figure 5). The X-ray diffraction pattern of the MQATPE + Eu-POM nanosheets displayed four clear peaks with d-spacings of 3.49, 1.65, 1.09, and 0.87 nm. These peaks can be indexed as the (001), (002), (003), and (004) diffractions of a lamellar structure, with a layer spacing of 3.49 nm. Combining the diameter of one Eu-POM (1.04 nm) and the length of two cationic MQATPE (3.68 nm, from the optimized structure of MQATPE in Figure S8), the ideal lamellar distance of MQATPE + Eu-POM is about 4.72 nm, which is much larger than the measured layer distance. We thus inferred that in the MQATPE + Eu-POM lamellar nanosheets, TPE groups would adopt a $\pi-\pi$ stacking and the alkyl chains possess a partial interdigitation.[36] This lamellar pattern is illustrated in Scheme 2a, in which the Eu-POM layers are alternated with the bilayer MQATPE.

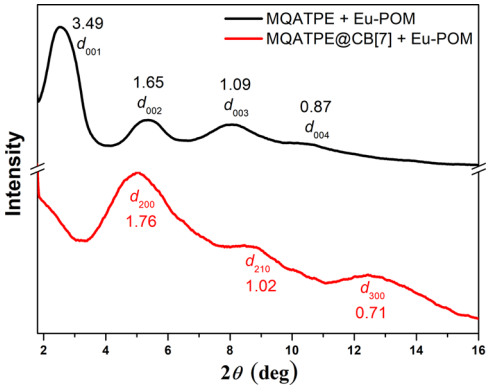

Figure 5. PXRD patterns of the MQATPE + Eu-POM nanosheets and MQATPE@CB[7] + Eu-POM hybrid films.

Interestingly, the XRD peaks of the MQATPE@CB[7] + Eu-POM films showed three clear Bragg diffractions with d-spacings at 1.76, 1.02, and 0.71 nm, equal to the ratio of $1:\sqrt{3}:2$, in agreement with the theoretical peak distribution of a hexagonal arrangement derived from Bragg's law.[37] Broad peaks were also observed at larger angles that correspond to d-spacings of approximately 0.41 and 0.33 nm (Figure S8), which could be assigned to the alkyl chain halo, $\pi-\pi$ stacking, and electrostatic interactions, indicating that there is a degree of ordering.[38] Considering the above bilayer spacing of 3.49 nm in the MQATPE + Eu-POM lamellar nanosheets, the first visible reflection at the d-spacing of 1.76 nm would correspond to the index of (200) within the hexagonal lattice, and then the first-order reflection along this axis (100) would have the d-spacing of 3.52 nm.[19] The unit lattice parameter a was calculated to be 4.06 nm given by $2d_{100}/\sqrt{3}$.[40,41] The increased value of a than the above layer distance of 3.49 nm could be attributed to the stiffening and stretching of the alkyl chain after being wrapped in CB[7]. In the control experiments using two-quaternary ammonium-modified TPE (TQATPE; Figure S9), three nearly identical Bragg diffractions of TQATPE@CB[7] + Eu-POM assembly were also observed with d-spacings equal to the ratio of $1:\sqrt{3}:2$, in agreement with the theoretical peak distribution of a hexagonal arrangement. Since there is only one TPE group in the TQATPE molecule, this observation demonstrated that the TPE groups of MQATPE would adopt a $\pi-\pi$ stacking in MQATPE@CB[7] + Eu-POM films, and the proposed hexagonal arrangement pattern is illustrated in Scheme 2b. For fabrication of large-area single-layer 2D films, the building block usually possesses a planar backbone and suppression of out-of-plane stacking of the backbone is also necessary.[12] The cyclic CB[7] groups bound on the alky chain would impose a steric influence on the arrangement of MQATPE around the Eu-POM. As the negative charges of Eu-POM are delocalized and moveable,[27] cationic MQATPE groups can spontaneously adjust their locations around the Eu-POM due to the electronic and steric effects; then, the triangular preorganized module was constructed. Due to the symmetrical and rigid stacking-forbidden properties, the constituent modules would adopt a single-layer 2D periodic hexagonal assembly via a $\pi-\pi$ stacking of the TPE groups.[27,19,42−44]

α-Chymotrypsin (ChT) is an important serine protease in the alimentary canal. As immoderate ChT activity may lead to serious medical disorders, modulation of ChT is of great importance in the field of biology. ChT can be inhibited through electrostatic interactions between ChT and the inhibitive materials, as the active site is surrounded by cations on the surface. The homogeneous MQATPE@CB[7] + Eu-POM single-layer films possess more accessible active sites (electronegative Eu-POM) than the aggregated nanosheets and would offer great opportunities to tune the enzyme activity. *N*-Succinyl-L-phenylalanine-*p*-nitroanilide (SPNA) as a substrate can be hydrolyzed to a product with a characteristic UV−vis absorption at 410 nm by ChT. To evaluate the inhibitory potency of the single-layer films, activity assays were conducted by preincubating ChT (80 $\mu g \cdot mL^{-1}$) and single-layer films with concentrations of Eu-POM ranging from 0 to

Scheme 2. Schematic Representation of the Self-Assembly Patterns of (a) MQATPE + Eu-POM Multilayer Nanosheets and (b) MQATPE@CB[7] + Eu-POM Hybrid Single-Layer Films

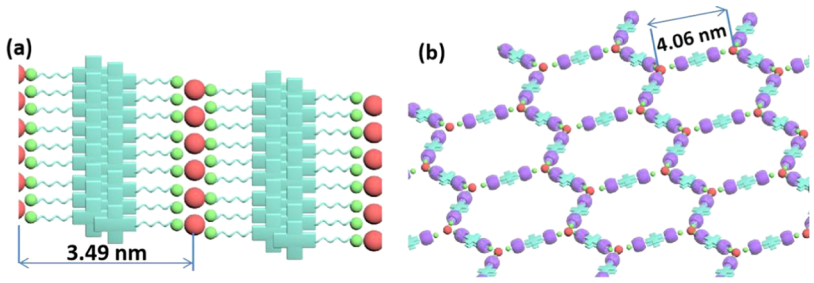

https://dx.doi.org/10.1021/acsami.0c02976
ACS Appl. Mater. Interfaces 2020, 12, 15615−15621

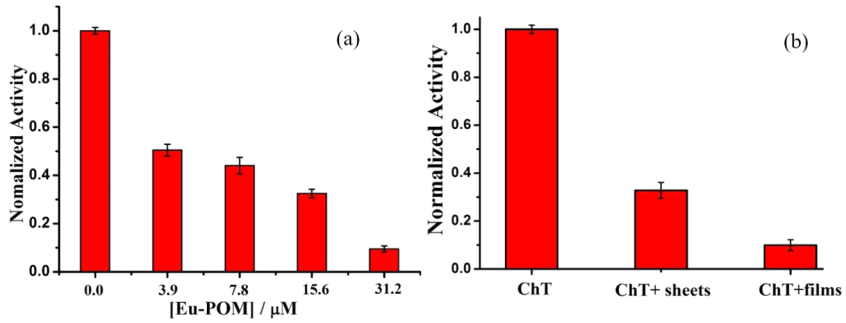

Figure 6. (a) Activity of ChT with different concentrations of single-layer films, calculated as a concentration of Eu-POM. (b) Activity of ChT with nanosheets and single-layer films (with the same concentrations of Eu-POM at 31.2 μM). The activities were normalized to that of ChT, and incubation time was maintained at 60 min.

31.2 μM. By monitoring the hydrolysis rate of SPNA and normalizing to the sample without inhibitors as control, the enzyme activities were determined. A remarkable decrease in the ChT activity was observed with the increasing concentration of the MQATPE@CB[7] + Eu-POM single-layer films and the activity was inhibited to 9% with films at a concentration of 31.2 μM Eu-POM (Figure 6a). The self-assembled single-layer films showed a superior inhibition effect compared to those of dendrimers,[45] carbon nanotubes,[46] gold nanoparticles,[47] and other materials.[48] We also tested the ChT activity with the incubation of the MQATPE + Eu-POM nanosheets. Inhibition efficiency shows a significant decrease with the incubation of nanosheets compared with that of single-layer films with the same Eu-POM concentration (Figure 6b). This might be ascribed to the good dispersibility and large surface areas of single-layer films for adequate protein binding.

CONCLUSIONS

In summary, we have successfully constructed hybrid single-layer films through a supramolecular approach by TPE derivatives, POM, and CB[7]. The assembly modes of MQATPE + Eu-POM and MQATPE@CB[7] + Eu-POM were unambiguously elucidated by fluorescence experiments, SEM, AFM, TEM, and XRD. White light with nearly ideal CIE coordinates has been obtained through the regulation of the contents of Eu-POM and MQATPE. We have also demonstrated MQATPE@CB[7] + Eu-POM single-layer films to be new protein inhibitors. Such a novel and simple strategy to build hybrid organic−inorganic single-layer frameworks via supramolecular interaction can be hopefully extended to diverse 2D supramolecular materials and may hold promise for practical applications in various areas such as membrane and biology.

ASSOCIATED CONTENT

Supporting Information

The Supporting Information is available free of charge at https://pubs.acs.org/doi/10.1021/acsami.0c02976.

Reagents and materials, methods and characterizations, fabrication of the 2D materials, the activity of ChT, fluorescence spectra, SEM and AFM images, EDX spectrum of MQATPE@CB[7] + Eu-POM films, FTIR and Raman spectra, and PXRD patterns (PDF)

AUTHOR INFORMATION

Corresponding Author

Yu Liu − *College of Chemistry, State Key Laboratory of Elemento-Organic Chemistry, Nankai University, Tianjin 300071, P. R. China; Collaborative Innovation Center of Chemical Science and Engineering (Tianjin), Tianjin 300071, P. R. China;* orcid.org/0000-0001-8723-1896; Email: yuliu@nankai.edu.cn

Authors

Ni Cheng − *College of Pharmacy, Weifang Medical University, Weifang, Shandong 261053, P. R. China; College of Chemistry, State Key Laboratory of Elemento-Organic Chemistry, Nankai University, Tianjin 300071, P. R. China*

Yong Chen − *College of Chemistry, State Key Laboratory of Elemento-Organic Chemistry, Nankai University, Tianjin 300071, P. R. China*

Yi Zhang − *College of Chemistry, State Key Laboratory of Elemento-Organic Chemistry, Nankai University, Tianjin 300071, P. R. China*

Complete contact information is available at: https://pubs.acs.org/10.1021/acsami.0c02976

Notes

The authors declare no competing financial interest.

ACKNOWLEDGMENTS

We thank NNSFC (21672113, 21432004, 21772099, 21861132001, 21901186, and 91527301) for financial support.

REFERENCES

(1) Fukui, T.; Kawai, S.; Fujinuma, S.; Matsushita, Y.; Yasuda, T.; Sakurai, T.; Seki, S.; Takeuchi, M.; Sugiyasu, K. Control over Differentiation of a Metastable Supramolecular Assembly in One and Two dimensions. *Nat. Chem.* **2017**, *9*, 493−499.

(2) Ma, R.; Sasaki, T. Two-Dimensional Oxide and Hydroxide Nanosheets: Controllable High-Quality Exfoliation, Molecular Assembly, and Exploration of Functionality. *Acc. Chem. Res.* **2015**, *48*, 136−143.

(3) Shen, J.; Liu, G.; Huang, K.; Jin, W.; Lee, K. R.; Xu, N. Membranes with Fast and Selective Gas-Transport Channels of Laminar Graphene Oxide for Efficient CO_2 Capture. *Angew. Chem.* **2015**, *127*, 588−592.

(4) Villalobos, L. F.; Huang, T.; Peinemann, K. V. Cyclodextrin Films with Fast Solvent Transport and Shape-Selective Permeability. *Adv. Mater.* **2017**, *29*, No. 1606641.

(5) Zhao, M.; Wang, Y.; Ma, Q.; Huang, Y.; Zhang, X.; Ping, J.; Zhang, Z.; Lu, Q.; Yu, Y.; Xu, H.; Zhao, Y.; Zhang, H. Ultrathin 2D

Metal−Organic Framework Nanosheets. *Adv. Mater.* **2015**, *27*, 7372−7378.
(6) Shi, Z.; Zhang, W.; Zhang, F.; Liu, X.; Wang, D.; Jin, J.; Jiang, L. Ultrafast Separation of Emulsified Oil/Water Mixtures by Ultrathin Free-Standing Single-Walled Carbon Nanotube Network Films. *Adv. Mater.* **2013**, *25*, 2422−2427.
(7) Dong, J.; Zhang, K.; Li, X.; Qian, Y.; Zhu, H.; Yuan, D.; Xu, Q. H.; Jiang, J.; Zhao, D. Ultrathin Two-Dimensional Porous Organic Nanosheets with Molecular Rotors for Chemical Sensing. *Nat. Commun.* **2017**, *8*, No. 1142.
(8) Baek, K.; Yun, G.; Kim, Y.; Kim, D.; Hota, R.; Hwang, I.; Xu, D.; Ko, Y. H.; Gu, G. H.; Suh, J. H.; Park, C. G.; Sung, B. J.; Kim, K. Free-Standing, Single-Monomer-Thick Two-Dimensional Polymers through Covalent Self-Assembly in Solution. *J. Am. Chem. Soc.* **2013**, *135*, 6523−6528.
(9) Bunck, D. N.; Dichtel, W. R. Bulk Synthesis of Exfoliated Two-Dimensional Polymers Using Hydrazone-Linked Covalent Organic Frameworks. *J. Am. Chem. Soc.* **2013**, *135*, 14952−14955.
(10) Payamyar, P.; Kaja, K.; Ruiz-Vargas, C.; Stemmer, A.; Murray, D. J.; Johnson, C. J.; King, B. T.; Schiffmann, F.; VandeVondele, J.; Renn, A.; Götzinger, S.; Ceroni, P.; Schütz, A.; Lee, L. T.; Zheng, Z.; Sakamoto, J.; Schlüter, A. D. Synthesis of a Covalent Monolayer Sheet by Photochemical Anthracene Dimerization at the Air/Water Interface and its Mechanical Characterization by AFM Indentation. *Adv. Mater.* **2014**, *26*, 2052−2058.
(11) He, P.; Xu, B.; Wang, P.; Liu, H.; Wang, X. A Monolayer Polyoxometalate Superlattice. *Adv. Mater.* **2014**, *26*, 4339−4344.
(12) Zhang, K. D.; Tian, J.; Hanifi, D.; Zhang, Y.; Sue, A. C.; Zhou, T. Y.; Zhang, L.; Zhao, X.; Liu, Y.; Li, Z. T. Toward a Single-Layer Two-Dimensional Honeycomb Supramolecular Organic Framework in Water. *J. Am. Chem. Soc.* **2013**, *135*, 17913−17918.
(13) O'Keeffe, M.; Yaghi, O. M. Deconstructing the Crystal Structures of Metal−Organic Frameworks and Related Materials into Their Underlying Nets. *Chem. Rev.* **2012**, *112*, 675−702.
(14) Yan, X.; Wang, F.; Zheng, B.; Huang, F. Stimuli-Responsive Supramolecular Polymeric Materials. *Chem. Soc. Rev.* **2012**, *41*, 6042−6065.
(15) Wang, J.; Huang, Z.; Ma, X.; Tian, H. Visible-Light-Excited Room-Temperature Phosphorescence in Water by Cucurbit[8]uril-Mediated Supramolecular Assembly. *Angew. Chem., Int. Ed.*. DOI: 10.1002/anie.201914513.
(16) Ma, X.; Wang, J.; Tian, H. Assembling-Induced Emission: An Efficient Approach for Amorphous Metal-Free Organic Emitting Materials with Room-Temperature Phosphorescence. *Acc. Chem. Res.* **2019**, *52*, 738−748.
(17) Zhang, H.; Liang, F.; Yang, Y. W. Dual-Stimuli Responsive 2D Supramolecular Organic Framework for the Detection of Azoreductase Activity. *Chem. Eur. J.* **2020**, *26*, 198−205.
(18) Li, Y. W.; Dong, Y. H.; Miao, X. R.; Ren, Y. L.; Zhang, B. L.; Wang, P. P.; Yu, Y.; Li, B.; Isaacs, L.; Cao, L. P. Shape-Controllable and Fluorescent Supramolecular Organic Frameworks Through Aqueous Host-Guest Complexation. *Angew. Chem., Int. Ed.* **2018**, *57*, 729−733.
(19) Pfeffermann, M.; Dong, R.; Graf, R.; Zajaczkowski, W.; Gorelik, T.; Pisula, W.; Narita, A.; Müllen, K.; Feng, X. Free-Standing Monolayer Two-Dimensional Supramolecular Organic Framework with Good Internal Order. *J. Am. Chem. Soc.* **2015**, *137*, 14525−14532.
(20) Zhang, C. C.; Zhang, Y. M.; Zhang, Z. Y.; Wu, X.; Yu, Q.; Liu, Y. Photoreaction-Driven Two-Dimensional Periodic Polyrotaxane-Type Supramolecular Nanoarchitecture. *Chem. Commun.* **2019**, *55*, 8138−8141.
(21) Zhou, W.; Chen, Y.; Dai, X.; Zhang, H. Y.; Liu, Y. Cucurbit[8]uril-Mediated Polypseudorotaxane for Enhanced Lanthanide Luminescence Behavior in Water. *Org. Lett.* **2019**, *21*, 9363−9367.
(22) Cheng, N.; Chen, Y.; Yu, J.; Li, J.-j.; Liu, Y. Photocontrolled Coumarin-diphenylalanine/Cyclodextrin Cross-Linking of 1D Nanofibers to 2D Thin Films. *ACS Appl. Mater. Interfaces* **2018**, *10*, 6810−6814.
(23) Zhang, C. C.; Zhang, Y. M.; Liu, Y. Photocontrolled Reversible Conversion of a Lamellar Supramolecular Assembly Based on Cucurbiturils and a Naphthalenediimide Derivative. *Chem. Commun.* **2018**, *54*, 13591−13594.
(24) Li, B.; Li, W.; Li, H.; Wu, L. Ionic Complexes of Metal Oxide Clusters for Versatile Self-Assemblies. *Acc. Chem. Res.* **2017**, *50*, 1391−1399.
(25) Li, H.; Qi, W.; Li, W.; Sun, H.; Bu, W.; Wu, L. A Highly Transparent and Luminescent Hybrid Based on the Copolymerization of Surfactant-Encapsulated Polyoxometalate and Methyl Methacrylate. *Adv. Mater.* **2005**, *17*, 2688−2692.
(26) Yan, X.; Zhu, P.; Fei, J.; Li, J. Self-Assembly of Peptide-Inorganic Hybrid Spheres for Adaptive Encapsulation of Guests. *Adv. Mater.* **2010**, *22*, 1283−1287.
(27) Yue, L.; Wang, S.; Zhou, D.; Zhang, H.; Li, B.; Wu, L. Flexible Single-Layer Ionic Organic-Inorganic Frameworks Towards Precise Nano-Size Separation. *Nat. Commun.* **2016**, *7*, No. 10742.
(28) Sugeta, M.; Toshihiro, Y. Crystal Structure and Luminescence Site of $Na_9[EuW_{10}O_{36}]\cdot 32H_2O$. *Bull. Chem. Soc. Jpn.* **1993**, *66*, 444−449.
(29) Jiang, B. P.; Guo, D. S.; Liu, Y. C.; Wang, K. P.; Liu, Yu. Photomodulated Fluorescence of Supramolecular Assemblies of Sulfonatocalixarenes and Tetraphenylethene. *ACS Nano* **2014**, *8*, 1609−1618.
(30) Barrow, S. J.; Kasera, S.; Rowland, M. J.; del Barrio, J.; Scherman, O. A. Cucurbituril-Based Molecular Recognition. *Chem. Rev.* **2015**, *115*, 12320−12406.
(31) Xu, S. Q.; Zhang, X.; Nie, C. B.; Pang, Z. F.; Xu, X. N.; Zhao, X. The Construction of a Two-Dimensional Supramolecular Organic Framework with Parallelogram Pores and Stepwise Fluorescence Enhancement. *Chem. Commun.* **2015**, *51*, 16417−16420.
(32) Zhang, J.; Liu, Y.; Li, Y.; Zhao, H.; Wan, X. Hybrid Assemblies of Eu-Containing Polyoxometalates and Hydrophilic Block Copolymers with Enhanced Emission in Aqueous Solution. *Angew. Chem., Int. Ed.* **2012**, *51*, 4598−4602.
(33) Nogami, M.; Abe, Y. Properties of Sol-Gel-Derived Al_2O_3-SiO_2 Glasses using Eu^{3+} Ion Fluorescence Spectra. *J. Non-Cryst. Solids* **1996**, *197*, 73−78.
(34) Wen, Y.; Sheng, T.; Zhu, X.; Zhuo, C.; Su, S.; Li, H.; Hu, S.; Zhu, Q. L.; Wu, X. Introduction of Red-Green-Blue Fluorescent Dyes into a Metal-Organic Framework for Tunable White Light Emission. *Adv. Mater.* **2017**, *29*, No. 1700778.
(35) Wang, Z.; Zhang, R.; Ma, Y.; Peng, A.; Fu, H.; Yao, J. Chemically Responsive Luminescent Switching in Transparent Flexible Self-Supporting $[EuW_{10}O_{36}]^{9-}$-Agarose Nanocomposite Thin Films. *J. Mater. Chem.* **2010**, *20*, 271−277.
(36) Bu, W.; Li, H.; Sun, H.; Yin, S. Y.; Wu, L. X. Polyoxometalate-Based Vesicle and Its Honeycomb Architectures on Solid Surfaces. *J. Am. Chem. Soc.* **2005**, *127*, 8016−8017.
(37) Yang, Y.; Wang, Y.; Li, H.; Li, W.; Wu, L. Self-Assembly and Structural Evolvement of Polyoxometalate-Anchored Dendron Complexes. *Chem. Eur. J.* **2010**, *16*, 8062−8071.
(38) Foster, E. J.; Jones, R. B.; Lavigueur, C.; Williams, V. E. Structural Factors Controlling the Self-Assembly of Columnar Liquid Crystals. *J. Am. Chem. Soc.* **2006**, *128*, 8569−8574.
(39) Magnotti, E. L.; Hughes, S. A.; Dillard, R. S.; Wang, S.; Hough, L.; Karumbamkandathil, A.; Lian, T.; Wall, J. S.; Zuo, X.; Wright, E. R.; Conticello, V. P. Self-Assembly of an α-Helical Peptide into a Crystalline Two-Dimensional Nanoporous Framework. *J. Am. Chem. Soc.* **2016**, *138*, 16274−16282.
(40) Vinu, A.; Ariga, K.; Mori, T.; Nakanishi, T.; Hishita, S.; Golberg, D.; Bando, Y. Preparation and Characterization of Well-Ordered Hexagonal Mesoporous Carbon Nitride. *Adv. Mater.* **2005**, *17*, 1648−1652.
(41) Seiki, N.; Shoji, Y.; Kajitani, T.; Ishiwari, F.; Kosaka, A.; Hikima, T.; Takata, M.; Someya, T.; Fukushima, T. Rational Synthesis

of Organic Thin Films with Exceptional Long-Range Structural Integrity. *Science* **2015**, *348*, 1122.

(42) Zhang, L.; Zhou, T.-Y.; Tian, J.; Wang, H.; Zhang, D.-W.; Zhao, X.; Liu, Y.; Li, Z. T. A Two-Dimensional Single-Layer Supramolecular Organic Framework that is Driven by Viologen Radical Cation Dimerization and Further Promoted by Cucurbit[8]-uril. *Polym. Chem.* **2014**, *5*, 4715−4721.

(43) Zhang, Y.; Zhan, T.-G.; Zhou, T.-Y.; Qi, Q.-Y.; Xu, X.-N.; Zhao, X. Fluorescence Enhancement through the Formation of a Single-Layer Two-Dimensional Supramolecular Organic Framework and its Application in Highly Selective Recognition of Picric Acid. *Chem. Commun.* **2016**, *52*, 7588−7591.

(44) Lee, H. J.; Kim, H. J.; Lee, E. C.; Kim, J.; Park Soo, Y. Highly Luminescent and Water-Soluble Two-Dimensional Supramolecular Organic Framework: All-Organic Photosensitizer Template for Visible-Light-Driven Hydrogen Evolution from Water. *Chem. Asian. J.* **2018**, *13*, 390−394.

(45) Chiba, F.; Chou, T.; Twyman, L. J.; Wagstaff, M. Dendrimers as Size Selective Inhibitors to Protein−Protein Binding. *Chem. Commun.* **2008**, 4351−4353.

(46) Zhang, B.; Xing, Y.; Li, Z.; Zhou, H.; Mu, Q.; Yan, B. Functionalized Carbon Nanotubes Specifically Bind to α-Chymotrypsin's Catalytic Site and Regulate its Enzymatic Function. *Nano Lett.* **2009**, *9*, 2280−2284.

(47) You, C. C.; De, M.; Han, G.; Rotello, V. M. Tunable Inhibition and Denaturation of α-Chymotrypsin with Amino Acid-Functionalized Gold Nanoparticles. *J. Am. Chem. Soc.* **2005**, *127*, 12873−12881.

(48) Park, H. S.; Lin, Q.; Hamilton, A. D. Protein Surface Recognition by Synthetic Receptors: a Route to Novel Submicromolar Inhibitors for α-Chymotrypsin. *J. Am. Chem. Soc.* **1999**, *121*, 8−13.

https://dx.doi.org/10.1021/acsami.0c02976
ACS Appl. Mater. Interfaces 2020, 12, 15615−15621